1-10-2008

Probing the electronic and structural properties of doped aluminum clusters: MAl_{12}^- (M=Li, Cu, and Au)

R. Pal
University of Nebraska-Lincoln

Li-Feng Cui
Washington State University, Richland

Satya S. Bulusu
University of Nebraska-Lincoln, sbulusu@iiti.ac.in

Hua-Jin Zhai
Washington State University, Richland

Lai-Sheng Wang
Washington State University, Richland

See next page for additional authors

Probing the electronic and structural properties of doped aluminum clusters: MAl_{12}^- (M=Li, Cu, and Au)

R. Pal
Department of Chemistry, University of Nebraska-Lincoln, Lincoln, Nebraska 68588, USA and Nebraska Center for Materials and Nanoscience, University of Nebraska-Lincoln, Lincoln, Nebraska 68588, USA

Li-Feng Cui
Department of Physics, Washington State University, Richland, Washington 99354, USA and Chemical and Materials Sciences Division, Pacific Northwest National Laboratory, MS K8-88, P.O. Box 999, Richland, Washington 99352, USA

S. Bulusu
Department of Chemistry, University of Nebraska-Lincoln, Lincoln, Nebraska 68588, USA and Nebraska Center for Materials and Nanoscience, University of Nebraska-Lincoln, Lincoln, Nebraska 68588, USA

Hua-Jin Zhai and Lai-Sheng Wang[a)]
Department of Physics, Washington State University, Richland, Washington 99354, USA and Chemical and Materials Sciences Division, Pacific Northwest National Laboratory, MS K8-88, P.O. Box 999, Richland, Washington 99352, USA

X. C. Zeng[b)]
Department of Chemistry, University of Nebraska-Lincoln, Lincoln, Nebraska 68588, USA and Nebraska Center for Materials and Nanoscience, University of Nebraska-Lincoln, Lincoln, Nebraska 68588, USA

(Received 17 August 2007; accepted 11 October 2007; published online 11 January 2008)

Photoelectron spectroscopy (PES) is combined with theoretical calculations to investigate the electronic and atomic structures of three doped aluminum clusters, MAl_{12}^- (M=Li, Cu, and Au). Well-resolved PES spectra have been obtained at two detachment photon energies, 266 nm (4.661 eV) and 193 nm (6.424 eV). Basin-hopping global optimization method in combination with density-functional theory calculations has been used for the structural searches. Good agreement between the measured PES spectra and theoretical simulations helps to identify the global minimum structures. It is found that $LiAl_{12}^-$ (C_{5v}) can be viewed as replacing a surface Al atom by Li on an icosahedral Al_{13}^-, whereas Cu prefers the central site to form the encapsulated D_{3d}-Cu@Al_{12}^-. For $AuAl_{12}^-$ (C_1), Au also prefers the central site, but severely distorts the Al_{12} cage due to its large size. © *2008 American Institute of Physics*. [DOI: 10.1063/1.2805386]

I. INTRODUCTION

Aluminum-transition-metal alloys are known to form quasicrystals, which have rotational order but no translational symmetry.[1] Icosahedral units, such as M@Al_{12}, are often found in M–Al (M=W, Mn, Cr, Mo, Tc, and Re) quasicrystal alloys. These icosahedral units seem to exhibit significant stability and can be viewed as building blocks of the quasicrystals. In the gas phase, Al_{13}^- is well known to be an icosahedral cluster with high geometric stability and a closed electronic shell as well.[2–8] Doping aluminum clusters with other impurity atoms provides an additional degree of freedom to fabricate mixed clusters with unique and tunable electronic and chemical properties. Indeed, mixed aluminum clusters have been extensively studied over the past decade with the hope to discover novel cluster-assembled materials.[9–34]

The Al_{13}^- cluster anion owes its pronounced stability to the major electronic shell closing at 40 valence electrons and its high I_h symmetry. Al_{13} has a high electron affinity (EA) of 3.57 eV,[4,30] similar to that of Cl (3.61 eV), the highest EA among the elements in the periodic table.[35] Li and Wang[30] previously studied the doped clusters of $Al_{12}X^-$ (X=C,Ge,Sn,Pb) using photoelectron spectroscopy (PES) and showed that neutral clusters $Al_{12}X$ (X=Ge,Sn,Pb) all possess the I_h-X@Al_{12} structures with a large energy gap between their highest occupied molecular orbitals (HOMOs) and lowest unoccupied molecular orbitals (LUMOs). The PES pattern of $Al_{12}C^-$ was found to be distinctly different, confirming that it does not possess an I_h structure. A recent PES and photoionization spectroscopic study by Akutsu *et al.*[21] suggested that $Al_{12}B^-$, $Al_{12}P$, and $Al_{12}P^+$ also have the I_h-X@Al_{12} structures.

Theoretical studies of the 13-atom doped aluminum clusters MAl_{12} have also been reported previously.[13–17] Khanna *et al.*[15] performed a comparative study between Cu and K doped aluminum clusters MAl_n (M=Cu,K;n=11–14) and showed that the ionization potential of Cu

a)Electronic mail: ls.wang@pnl.gov.
b)Electronic mail: xczeng@phase2.unl.edu.

doped aluminum cluster is larger than that of K doped one. Because the atomic size of Cu and Al is close to each other, the copper dopant tends to locate at the central site inside the Al cage. In contrast, K dopant tends to locate outside the Al cage. Zope and Baruah[17] used B3LYP/LANL2DZ level of density-functional theory (DFT) and studied 13-atom aluminum clusters containing a metal dopant. They suggested that doping the cluster with the coinage metal or alkali metal atom results in a lower ionization potential and that the dopant atom prefers to stay at the periphery rather than at the center in both cases. The coinage metal atom doped clusters with the dopant atom at the center can be stable (local minima), but the low-lying isomers typically have the dopant at the periphery. The $CuAl_{12}$ cluster was investigated in more detail by Kumar and Kawazoe[13] and a highly symmetric structure (I_h point group) with a large magnetic moment was predicted.

In a series of previous work, we have studied the electronic and geometric structures of a variety of mixed aluminum clusters using PES and also in combination with *ab initio* calculations.[23–34] Well-resolved PES spectra serve as electronic "fingerprints" of the underlying clusters and can be used for comparisons with theoretical simulations. In the current contribution, we report on a joint PES and theoretical investigation of metal-doped aluminum cluster anions, MAl_{12}^- (M=Li, Cu, and Au). Good agreement between the measured PES spectra and the simulated ones enables us to identify the energetically most stable structures of MAl_{12}^- (M=Li, Cu, and Au).

II. EXPERIMENTAL AND THEORETICAL METHODS

A. Photoelectron spectroscopy

The experiments were carried out using a magnetic-bottle time-of-flight PES apparatus, details of which have been described elsewhere.[36] Briefly, aluminum/metal alloy clusters were produced by laser vaporization of a compressed disk target made from Al and M (M=Li, Cu, and Au). The laser-produced plasma was mixed with a helium carrier gas pulse at 10 atm backing pressure. A cold cluster beam was produced via supersonic expansion of clusters and carrier gas mixture through a 2 mm diameter nozzle and collimated by a 6 mm diameter skimmer. The cluster anions were extracted from the beam perpendicularly and analyzed by a time-of-flight mass spectrometer. The MAl_{12}^- (M=Li, Cu, and Au) cluster anions of interest were each mass selected and decelerated before crossing with a detachment laser beam in the interaction zone of the magnetic-bottle PES analyzer. Photoelectrons were collected at nearly 100% efficiency by the magnetic bottle and analyzed in a 3.5-m-long electron flight tube. The binding energy spectra were obtained by subtracting the kinetic energy spectra from the photon energies of the detachment laser. In the current study, two detachment photon energies were used, 266 nm (4.661 eV) from a Nd:yttrium aluminum garnet laser and 193 nm (6.424 eV) from an ArF excimer laser. The PES spectra were calibrated using the known spectra of Au^- at 193 nm and Pt^- at 266 nm. The PES apparatus had an electron energy resolution of $\Delta E/E \approx 2.5\%$, that is, ~25 meV for 1 eV electrons.

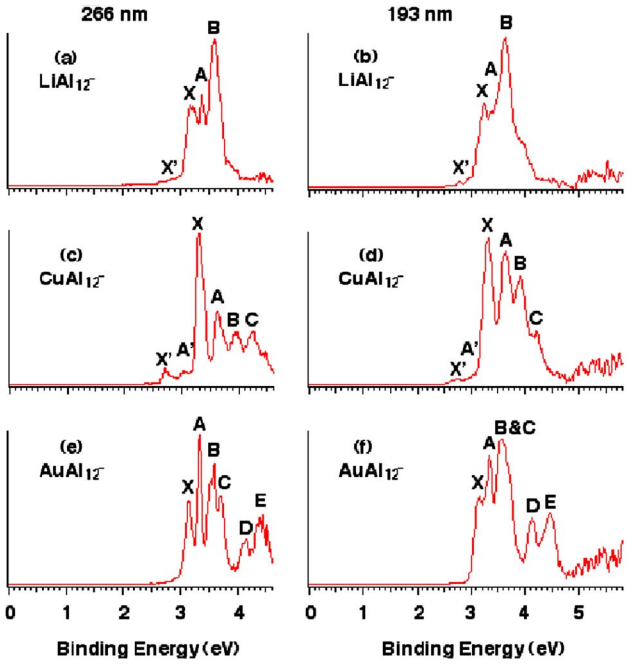

FIG. 1. (Color online) Photoelectron spectra of MAl_{12}^- (M=Li, Cu, and Au) at 266 nm (4.661 eV) and 193 nm (6.424 eV).

B. Theoretical methods

For all the doped clusters we employed the basin-hopping (BH) global optimization technique combined with DFT calculations to search the global-minimum structures.[37] The BH method essentially converts the potential energy surface ($\tilde{E}$) to a multidimensional "staircase" via the mapping $\tilde{E}(\mathbf{X})=\min\{E(\mathbf{X})\}$, where $\mathbf{X}$ denotes the nuclear coordinates of the cluster and "min" refers to the energy minimization performed starting from $\mathbf{X}$.[38] In practice, the canonical Monte Carlo (MC) sampling method was used to explore the transformed potential energy surface $\tilde{E}$ at a fixed temperature. With each MC move, coordinates of all atoms are randomly displaced, followed by a geometry optimization using a DFT method. Specifically, the DFT method with gradient-corrected Perdue-Burke-Ernzerhof (PBE) exchange correlation functional,[39] which is implemented in the DMOL3 program,[40] was employed for the structural optimization.

Unbiased BH searches were performed for all the clusters, MAl_{12}^- (M=Li, Cu, and Au). Despite marked differences among the randomly generated initial structures of a cluster, the BH-DFT search consistently yields the same lowest-energy isomer, typically within 200 MC trial moves. Among the top low-lying isomers, those having energy values within 0.2 eV from the lowest-lying isomer were regarded as candidates for the lowest-energy structure, whose simulated spectra are to be compared with the experimental PES data. Relative energies of the candidate isomers (three for the Li doped cluster, and six each for the Cu and Au doped clusters) with respect to the lowest-energy isomer were further evaluated using PBE functional with 6-31G(d) (for Al, Li, and Cu) or LANL2DZ (for Au) basis sets,[41] which are implemented in the GAUSSIAN 03 software package.[42] Vibrational frequency calculations were also carried out for all the optimized clusters to ascertain the absence of imaginary frequen-

TABLE I. Experimental ADE and VDE for MAl_{12}^- (M=Li, Cu, and Au) and theoretical VDEs for the lowest energy isomers calculated at the PBEPBE/6-31G(d) level for the Cu and Li doped clusters and PBEPBE/LANL2DZ level for Au doped cluster.

Species	ADE (expt., eV)	VDE (expt., eV)	Point group	VDE (theoretical, eV)
$LiAl_{12}^-$	3.10±0.05	3.23±0.05	C_{5v}	3.12
$CuAl_{12}^-$	3.24±0.03	3.31±0.03	D_{3d}	3.15
$AuAl_{12}^-$	3.10±0.05	3.15±0.03	C_1	3.08

cies. Finally, simulated PES spectra for all candidate isomers were obtained, for which the first vertical detachment energies (VDEs) of all the isomers were calculated as the energy difference between the ground state of the anion and that of the neutral cluster at the geometry of the anion. The binding energies of the deeper orbitals were then added to the first VDE to give the electronic density of states. Each calculated VDE was fitted with a Gaussian of width 0.04 eV to give the simulated spectra, which are compared to the experimental PES spectra.

III. EXPERIMENTAL RESULTS

The measured PES spectra of MAl_{12}^- (M=Li, Cu, and Au) at 266 and 193 nm detachment photon energies are shown in Fig. 1. Although the three species have the same number of valence electrons, their PES spectra are quite different from each other, suggesting they should possess different structures. The 193 nm spectrum of $LiAl_{12}^-$ [Fig. 1(b)] shows congested bands between 3 and 4 eV and displays no intense electronic transitions at higher binding energies. The 266 nm spectrum [Fig. 1(a)] resolves the spectrum within the same binding energy regime into three major bands (labeled X, A, and B). The X band represents the ground state transition, yielding adiabatic detachment energy (ADE) and VDE of 3.10 and 3.23 eV, respectively. A low binding energy tail (labeled X') was observed in both the 193 and 266 nm spectra, indicating the existence of minor isomers.

The spectra of $CuAl_{12}^-$ exhibit four well-resolved bands between 3 and 4.3 eV [Figs. 1(c) and 1(d)]. The ground state transition (X) in the 266 nm spectrum yields an ADE and VDE as 3.24 and 3.31 eV, respectively. Minor features X' and A' at the low binding energies of 2.71 and 3.05 eV, respectively, were quite prominently observed in the 266 nm spectrum, which are attributed to low-lying isomers.

The spectra of $AuAl_{12}^-$ [Figs. 1(e) and 1(f)] were well resolved with numerous features, which appear to consist of four relatively sharp bands (X,$A-C$) between 3 and 3.8 eV and two broader bands (D and E) at 4.15 and 4.45 eV. The ground state transition defined by band X yields an ADE and VDE of 3.10 and 3.15 eV, respectively. The sharp peak X also suggests that there is no significant geometry change between the ground states of $AuAl_{12}^-$ and $AuAl_{12}$. The measured ADEs and VDEs for all three clusters are summarized in Table I and compared with the calculated VDEs.

IV. THEORETICAL RESULTS

The low-lying structures located for MAl_{12}^- (M=Li, Cu, and Au) are depicted in Figs. 2–4, respectively. The calculated ground state VDEs are compared with the experimental data in Table I. The symmetries, total energies, relative energies, and HOMO-LUMO gaps of all low-lying structures are summarized in Table II. The simulated PES spectra for all low-lying structures are shown in Figs. 5–7.

TABLE II. Symmetry, total energy (DFT), relative energy (DFT), and HOMO-LUMO gaps for each of the three low-lying isomers of $LiAl_{12}^-$ and the six low-lying isomers of $CuAl_{12}^-$ and $AuAl_{12}^-$. The lowest-energy isomers are denoted in bold.

Species	Point group	Energy (a.u.)	ΔE (eV)	HOMO-LUMO gap (eV)
$LiAl_{12}^-$(1)	**C_{5v}**	**−2915.237 435 38**	**0.000**	**0.792**
$LiAl_{12}^-$(2)	C_s	−2915.222 540 53	0.405	0.872
$LiAl_{12}^-$(3)	C_s	−2915.222 582 40	0.404	0.738
$CuAl_{12}^-$(1)	**D_{3d}**	**−4547.786 228 00**	**0.000**	**0.317**
$CuAl_{12}^-$(2)	C_s	−4547.782 541 79	0.099	0.696
$CuAl_{12}^-$(3)	C_1	−4547.776 544 28	0.263	0.869
$CuAl_{12}^-$(4)	C_1	−4547.772 161 90	0.383	1.178
$CuAl_{12}^-$(5)	C_s	−4547.769 629 69	0.452	0.838
$CuAl_{12}^-$(6)	C_s	−4547.763 905 42	0.607	0.860
$AuAl_{12}^-$(1)	**C_1**	**−159.786 211 128**	**0.000**	**1.004**
$AuAl_{12}^-$(2)	C_s	−159.783 342 294	0.078	0.921
$AuAl_{12}^-$(3)	C_s	−159.777 941 918	0.225	0.914
$AuAl_{12}^-$(4)	C_s	−159.775 957 450	0.279	0.845
$AuAl_{12}^-$(5)	C_1	−159.769 350 826	0.459	0.895
$AuAl_{12}^-$(6)	C_s	−159.767 586 152	0.507	0.737

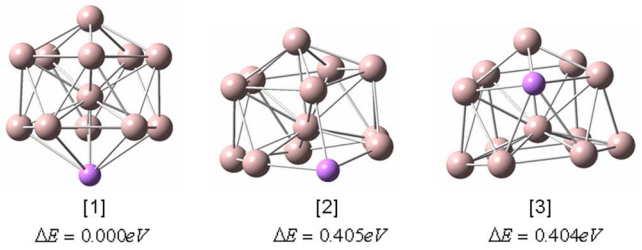

FIG. 2. (Color online) Structures and relative energies of the three low-lying isomers of $LiAl_{12}^-$. Aluminum atoms are larger spheres and in light purple.

A. $LiAl_{12}^-$

For $LiAl_{12}^-$, the BH search yielded three low-lying structures (Fig. 2). The electronic energies (in hartree) of all three isomers, calculated at PBEPBE/6-31G(d) level of theory, are listed in Table II. The lowest-energy structure possesses C_{5v} symmetry and can be viewed as replacing a surface Al atom by Li in the I_h-Al_{13}^-. The C_{5v}-$LiAl_{12}^-$ possesses two types of Li–Al bonds (5×2.91 and 1×2.59 Å). Our results for $LiAl_{12}^-$ are consistent with those obtained by Majumder *et al.*[10] Alternative structures 2 and 3 are distorted with low symmetry (C_s) and are ~0.4 eV higher in energy than the C_{5v} structure. In all structures (1–3), the Li atom occupies a surface rather than interior site.

B. $CuAl_{12}^-$

The BH search yielded six low-lying isomers for $CuAl_{12}^-$, as shown in Fig. 3 and Table II. The lowest-energy structure possesses D_{3d} symmetry with the Cu atom located inside the Al_{12} cage. Note that the structure of the lowest-energy neutral isomer reported by Kumar and Kawazoe[13] was more symmetric (I_h point group). Our global minimum search yielded a slightly lower symmetry (D_{3d}) for the anion isomer, reminiscent of a Jahn-Teller distortion from the I_h cluster. The structure of isomer 2 reveals a proximity to that of the highly symmetric isomer 1, but all other isomers (3–6) are highly distorted with an open aluminum cage structure. The Cu atom occupies the interior site in structures 1–3, whereas it occupies a surface site in structures 4–6.

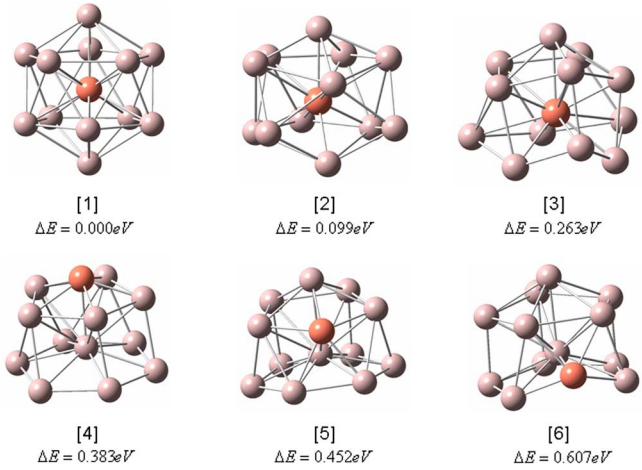

FIG. 3. (Color online) Structures and relative energies of the six low-lying isomers of $CuAl_{12}^-$. Aluminum atoms are shown in light purple.

C. $AuAl_{12}^-$

Similar to the Cu-doped cluster, the BH search yielded also six low-lying isomers for $AuAl_{12}^-$, as shown in Fig. 4. The electronic energies (in hartree) and relative energies of all the six isomers, calculated at the PBEPBE/LANL2DZ level of theory, are listed in Table II. Unlike the Cu-doped cluster, the lowest-energy isomer of $AuAl_{12}^-$ (isomer 1) exhibits low-symmetry (C_1) with an interior Au atom. Isomer 2, which also features an interior Au atom, is close in energy; but in all other isomers (3–6) the Au atom is outside the aluminum cage. All the $AuAl_{12}^-$ isomers possess low symmetry (C_1 or C_s) and open aluminum cages due to the large size of the dopant atom.

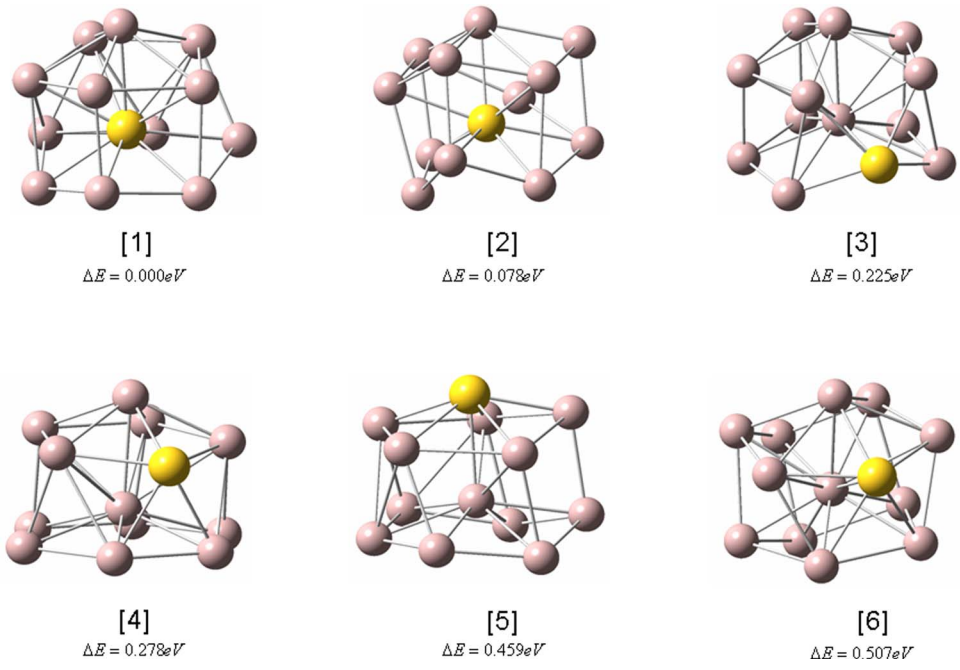

FIG. 4. (Color online) Structures and relative energies of the six low-lying isomers of $AuAl_{12}^-$. Aluminum atoms are shown in light purple.

V. DISCUSSION

A. Comparison between experiment and theory and confirmation of the ground state structures

The well-resolved PES spectra for MAl_{12}^- (M=Li, Cu, and Au) as shown in Fig. 1 serve as definitive electronic fingerprints, which allow detailed comparisons with the computational simulations to locate the ground state structures of the clusters. The calculated ground state VDEs for the lowest-energy isomer in each species are compared with experimental data in Table I. The computational data are 0.07–0.16 eV within the experimental measurements, which should be considered excellent agreement.

The simulated PES spectra for all the low-lying isomers of the doped clusters are shown in Figs. 5–7, respectively. We found that in each case the simulated spectrum for the global-minimum structure agrees best with the experimental spectrum, in particular for the transitions below ~4.5 eV. In the simulated spectra, there are clear transitions in the higher binding energy range beyond 5 eV. In the experimental spectra at 193 nm, weak signals are indeed present in the higher binding energy range, but they appear very weak and not well defined. It is conceivable that in the higher energy range the simple molecular orbital picture is no longer fitting to describe the photoemission processes. This is likely to be the case for all three clusters and we will only focus on the more intense features at the lower binding energy side in the comparison between experimental and simulated PES spectra.

Isomer 1 for $LiAl_{12}^-$ clearly gives a well-matched PES pattern as compared to the experiment data. The three experimental PES bands between 3 and 4 eV [Figs. 1(a) and 1(b)] are roughly reproduced computationally [Fig. 5(a)]. On the other hand, the simulated spectra for isomers 2 and 3 do not agree with the experimental spectra. They both give relatively low electron binding energies, and their simulated spectra are congested at below 4 eV, in contrast to the relatively simple experimental PES pattern. Thus, isomers 2 and 3 should have negligible contributions to the PES spectra.

For $CuAl_{12}^-$, the lowest energy isomer 1 [Fig. 6(a)] gives very good match to the experimental spectra [Figs. 1(c) and 1(d)] and the VDE is also in good agreement with the experimental spectra. In particular, the four well-resolved PES bands (*X*, *A*, *B*, *C*) between 3 and 4.3 eV are well reproduced by isomer 1. All other structures (2–6) generate too many PES features and congested PES patterns within this binding energy regime, in disagreement with the experimental data. Thus the observed PES pattern for $CuAl_{12}^-$ is relatively simple and in accord with the high symmetry structure 1.

The situation for $AuAl_{12}^-$ appears to be more complex (Fig. 7). All six structures produce similar ground state VDEs close to the experimental data, with structures 4 and 5 being slightly worse. In terms of the overall PES pattern, those of structures 2 and 5 appear to be diffuse, in disagreement with the experimental data. Furthermore, structure 3 generates doublet peaks at the lowest binding energies, also in disagreement with the observed sharp ground state feature *X* [Fig. 1(e)]. Structure 6 is ~0.5 eV higher in energy than the ground state and its contribution to the PES spectra should be negligible. Therefore, structure 1 is the best candidate to interpret the PES spectra for $AuAl_{12}^-$.

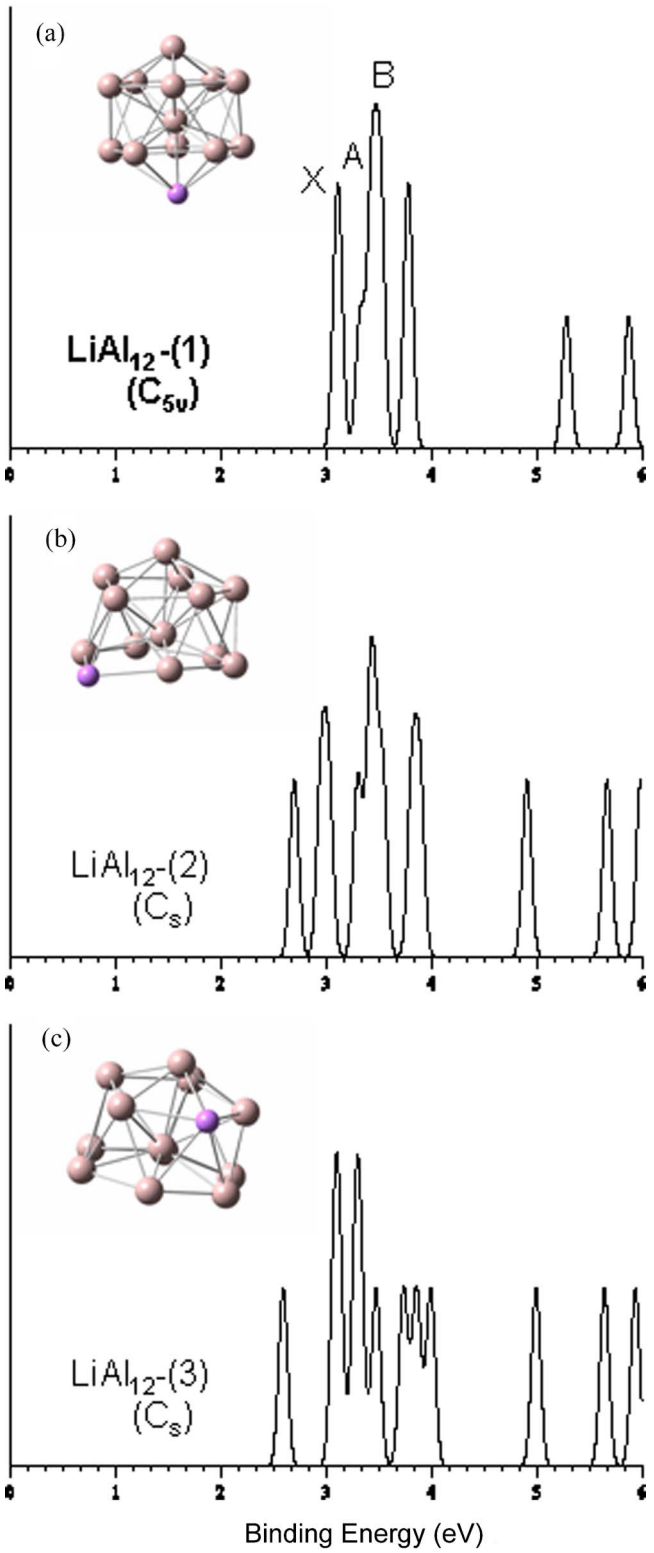

FIG. 5. (Color online) [(a)–(c)] Simulated spectra of the three low-lying isomers of $LiAl_{12}^-$ obtained from BH search.

B. On the minor isomers in $LiAl_{12}^-$ and $CuAl_{12}^-$

The weak low binding energy tails (*X'*) observed in $LiAl_{12}^-$ [Figs. 1(a) and 1(b)] and $CuAl_{12}^-$ [Figs. 1(c) and 1(d)]

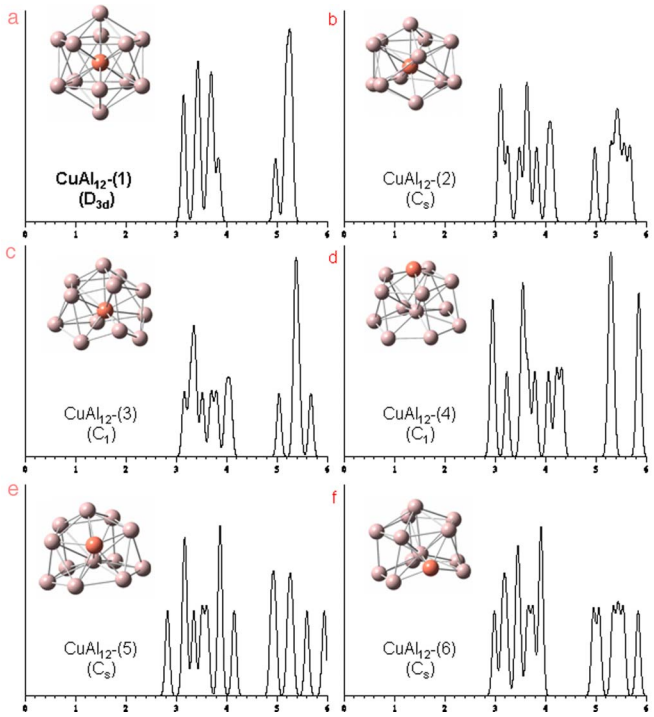

FIG. 6. (Color online) [(a)–(f)] simulated spectra of the six low-lying isomers of $CuAl_{12}^-$ obtained from BH search.

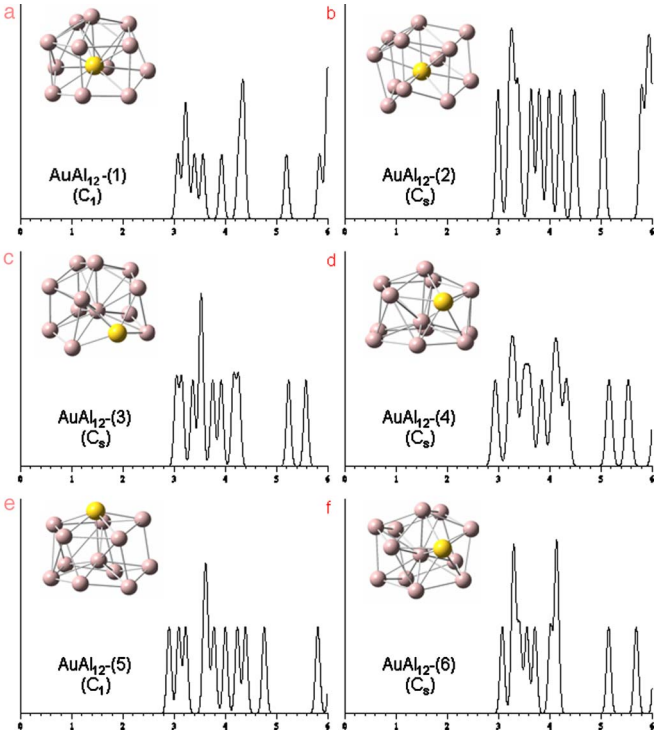

FIG. 7. (Color online) [(a)–(f)] simulated spectra of the six low-lying isomer of $AuAl_{12}^-$ obtained from BH search.

suggest that minor isomers are populated in the corresponding cluster beams. The experimental data can be best viewed in the perspective of presence of different spin states of the lowest lying isomer 1 (Tables III and IV). However, due to the complexity of the system, this interpretation may be considered tentative.

According to the concept of jellium model[43] the valence orbitals of all these clusters can be triply degenerate ($2p$). Therefore the anion and neutral isomers can acquire singlet/triplet and/or doublet/quartet spin states, respectively. Kumar and Kawazoe[13] suggested a higher spin quartet state (three unpaired electrons; M=4) for the neutral $CuAl_{12}$ cluster, which led us to recalculate the energies of all the plausible spin states for all the lowest-energy isomers and to compare their spectra for matching the minor features in the experimental spectra. All the spin states of the lowest-lying isomer were reoptimized using both DFT and Møller-Plesset second-order (MP2) perturbation theory[44] and 6-31G(d) basis sets. The relative energies of the lowest energy isomers at several spin states are given in Table III. Table IV compares the experimental (feature X' in Fig. 1) and theoretical VDEs of both Li and Cu doped species. Although the triplet state has high energy it may still be considered as a metastable state for isomer 1 and possibly gives rise to the minor features (e.g., feature X') in the spectra owing to a very low population (Fig. 8).

A careful analysis of the weak X' feature in the spectrum of $LiAl_{12}^-$ revealed two distinct transitions (2.79, 2.98 eV) which are extremely near to the features generated by the simulated PES (2.71, 3.06 eV) of the triplet ground state of the anion to a doublet excited state of the neutral of the

TABLE III. Relative energies (in eV) of the different spin states from DFT-PBE, MP2, and CCSD(T) calculations of all lowest-lying isomers. M denotes the spin multiplicity of the isomer. Spin states with very close energies are highlighted in bold.

	Anion			Neutral (in anion geometry)		
Species		DFT	MP2 [CCSD(T)]		DFT	MP2
$LiAl_{12}$	Singlet (M=1)	0.000		Doublet (M=2)	0.000	0.000
	Triplet (M=3)	0.415		Quartet (M=4)	0.409	0.270
$CuAl_{12}$	Singlet (M=1)	**0.061**	0.000 [0.000]	Doublet (M=2)	**0.000**	0.000
	Triplet (M=3)	**0.000**	0.294 [0.237]	Quartet (M=4)	**0.094**	0.190
$AuAl_{12}$	Singlet (M=1)	0.000		Doublet (M=2)	0.000	0.000
	Triplet (M=3)	0.533		Quartet (M=4)	0.572	0.323

TABLE IV. Experimental VDE for the minor isomer in the PES of $LiAl_{12}^-$ and $CuAl_{12}^-$ (X' in Fig. 1) and the calculated VDE with the triplet spin anions.

Species	VDE (expt., eV)	VDE (theoretical, eV)
$LiAl_{12}^-$	2.79±0.05	2.710
$CuAl_{12}^-$	2.71±0.03	2.707

isomer 1. In a previous PES study, Thomas *et al.* recorded a 355 nm spectrum for $LiAl_{12}^-$ at a lower resolution and reported an EA of 2.40±0.20 eV for $LiAl_{12}$,[16] which appears to be due to the minor isomer with a higher spin. Our current PES data indicate the $LiAl_{12}$ ground state possesses a substantially higher EA of 3.10±0.05 eV (Table I).

For $CuAl_{12}^-$, the presence of low-lying isomers in the experiment was more prominent [X' and A' in Fig. 1(c)]. The different spin states of this isomer were also reoptimized using the MP2 level of theory and 6-31G(d) basis sets. Subsequent single-point energy calculation at the coupled-cluster level of theory (including singles, doubles, and noniterative perturbative triples) CCSD(T) and 6-311+G(2d) basis sets showed that the triplet-state isomer is actually higher in energy than the singlet-state isomer (Table III). Hence, the probable weak features (X' and A') were most likely due to transitions from a triplet anion to a doublet neutral state (Fig. 8). Since the triplet anion state in this case is closer in energy to the corresponding singlet, the triplet-state isomer should have a slightly higher population, compared to the higher-spin isomers in $LiAl_{12}^-$ for contribution to the minor feature X' (Table III). Moreover, the quartet neutral state is much closer in energy to the doublet. This relatively small energy difference will influence the population of each state and therefore can be held responsible for the triplet to doublet state transition of the Cu doped species. The VDE for the minor isomer of $CuAl_{12}^-$ is measured to be 2.71±0.03 eV (Table IV), which is ~0.6 eV lower than that of the main isomer. Thomas *et al.* previously reported an electron affinity of 2.53 eV for $CuAl_{12}$ on the basis of a PES measurement at 355 nm.[12] Again, this number should be attributed to the minor isomer with a higher spin. The electron affinity for the $CuAl_{12}$ ground state is 3.24±0.03 eV (Table I).

For $AuAl_{12}^-$ the MP2 level calculation was generally consistent with DFT calculations for the isomer 1. The weak features arising from different spin states as in the case for Li and Cu doped species were not very prominent in the case of $AuAl_{12}^-$ (Fig. 1). Table III shows that the triplet anion isomer is much higher in energy compared to the corresponding singlet one. This large energy difference is also consistent for the spin states of the neutral isomers, i.e., the quartet one is much higher in energy than the corresponding doublet state for $AuAl_{12}$. In summary, the triplet and quartet spin states of $AuAl_{12}^-/AuAl_{12}$ are almost equally high in energy (Fig. 8)

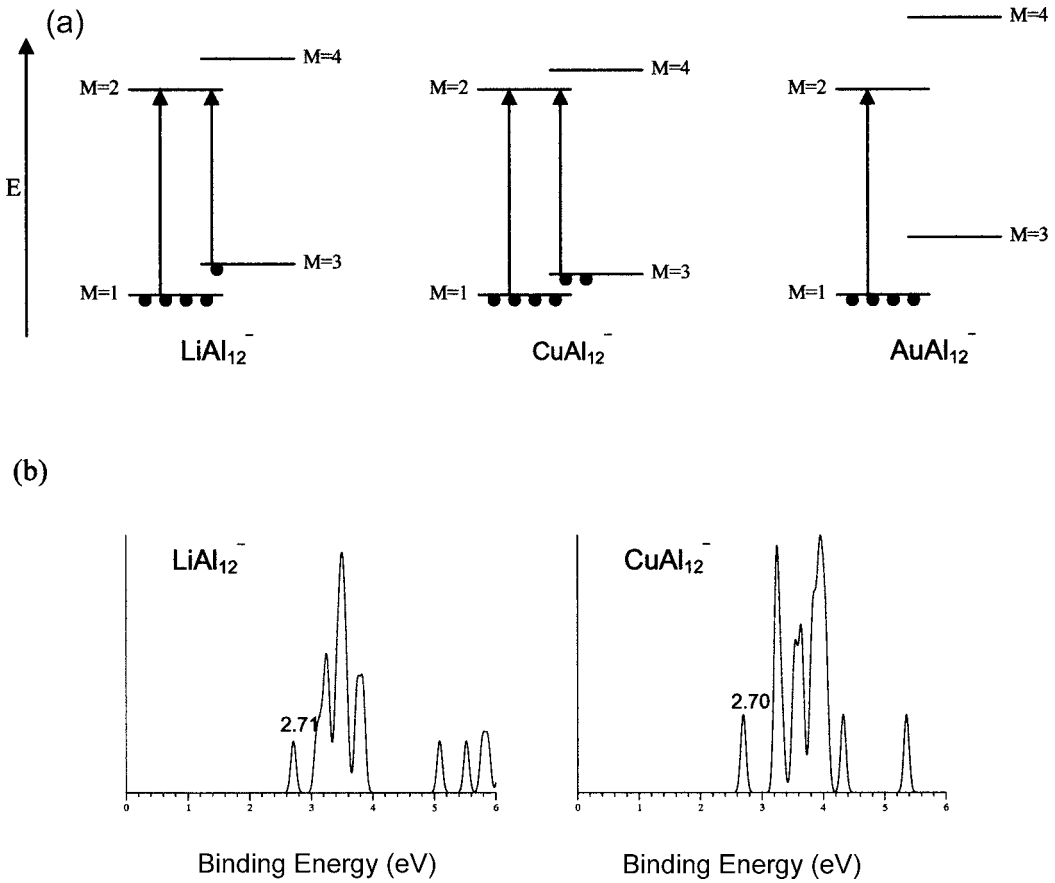

FIG. 8. (a) Relative energies of different spin states and all the probable transitions for Li, Cu, and Au doped species. The solid dots schematically show the population of MAl_{12}^- (M=Li, Cu, and Au) in different spin states. (b) The calculated spectra based on the triplet to doublet state transition in the cases of $LiAl_{12}^-$ and $CuAl_{12}^-$.

and therefore the lack of their population might be responsible for the almost absence of minor features in the experimental spectra.

VI. CONCLUSIONS

In conclusion, we have conducted a combined photoelectron spectroscopy and computational study on a series of doped aluminum clusters, MAl_{12}^- (M=Li, Cu, and Au). Well-resolved PES spectra were obtained at two detachment photon energies, 266 nm (4.661 eV) and 193 nm (6.424 eV), revealing electronic as well as isomeric information. Basin-hopping global optimization method combined with density-functional theory calculations were used for the structural searches. Good agreement between the measured PES spectra and theoretical simulations lends considerable credence for the obtained global minimum structures for each doped cluster. It was found that $LiAl_{12}^-$ (C_{5v}) can be viewed as replacing a surface Al atom by Li on an icosahedral Al_{13}^-, whereas Cu prefers the central site to form the encapsulated D_{3d}-Cu@Al_{12}^-. For $AuAl_{12}^-$ (C_1), Au also prefers the central site, but severely distorts the Al_{12} cage due to its large size. The structural trend in this series may be understood on the basis of the atomic sizes of the dopants and their nature of chemical bonding.

ACKNOWLEDGMENTS

We thank Dr. Xi Li for his assistance during the experimental work. The theoretical work done at Nebraska was supported by grants from the DOE's Office of Basic Energy Sciences (Grant No. DE-FG02-04ER46164), National Science Foundation (Grant Nos. CHE-0427746 and CMMI-0709333), the Nebraska Research Initiative, and the UNL Research Computing Facility. The experimental work done at Washington was supported by the National Science Foundation (Grant No. DMR-0503383) and the John Simon Guggenheim Foundation, and was performed at the EMSL, a national scientific user facility sponsored by the DOE's Office of Biological and Environmental Research and located at the Pacific Northwest National Laboratory, operated for DOE by Battelle.

[1] W. B. Pearson, *The Crystal Chemistry and Physics of Metals and Alloys* (Wiley, New York, 1972).
[2] R. E. Leuchtner, A. C. Harms, and A. W. Castleman, Jr., J. Chem. Phys. **94**, 1093 (1991).
[3] U. Röthlisberger, W. Andreoni, and P. Giannozzi, J. Chem. Phys. **96**, 1248 (1992).
[4] X. Li, H. B. Wu, X. B. Wang, and L. S. Wang, Phys. Rev. Lett. **81**, 1909 (1998).
[5] J. Akola, M. Manninen, H. Häkkinen, U. Landman, X. Li, and L. S. Wang, Phys. Rev. B **60**, R11297 (1999).
[6] R. Ahlrichs and S. D. Elliott, Phys. Chem. Chem. Phys. **1**, 13 (1999).
[7] D. E. Bergeron, A. W. Castleman, Jr., T. Morisato, and S. N. Khanna, Science **304**, 84 (2004); D. E. Bergeron, P. J. Roach, A. W. Castleman, Jr., N. O. Jones, and S. N. Khanna, *ibid.* **307**, 231 (2005).
[8] O. Dolgounitcheva, V. G. Zakrzewski, and J. V. Ortiz, J. Chem. Phys. **111**, 10762 (1999).
[9] J. Jellinek and E. B. Krissinel, Chem. Phys. Lett. **258**, 283 (1996); E. B. Krissinel and J. Jellinek, *ibid.* **272**, 301 (1997).
[10] C. Majumder, G. P. Das, S. K. Kulshrestha, V. Shah, and D. G. Kanhere, Chem. Phys. Lett. **261**, 515 (1996).
[11] X. G. Gong and V. Kumar, Phys. Rev. Lett. **70**, 2078 (1993); X. G. Gong and V. Kumar, Phys. Rev. B **50**, 17701 (1994); V. Kumar and V. Sundararajan, *ibid.* **57**, 4939 (1998).
[12] O. C. Thomas, W. Zheng, and K. H. Bowen, J. Chem. Phys. **114**, 5514 (2001).
[13] V. Kumar, Phys. Rev. B **57**, 8827 (1998); V. Kumar, *ibid.* **60**, 2916 (1999); V. Kumar and Y. Kawazoe, *ibid.* **64**, 115405 (2001).
[14] B. K. Rao and P. Jena, J. Chem. Phys. **115**, 778 (2001).
[15] S. N. Khanna, C. Ashman, B. K. Rao, and P. Jena, J. Chem. Phys. **114**, 9792 (2001).
[16] O. C. Thomas, W.-J. Zheng, T. P. Lippa, S.-J. Xu, S. A. Lyapustina, and K. H. Bowen, J. Chem. Phys. **114**, 9895 (2001).
[17] R. R. Zope and T. Baruah, Phys. Rev. A **64**, 053202 (2001).
[18] S. N. Khanna, B. K. Rao, and P. Jena, Phys. Rev. B **65**, 125105 (2002).
[19] O. P. Charkin, D. O. Charkin, N. M. Klimenko, and A. M. Mebel, Faraday Discuss. **124**, 215 (2003).
[20] Y.-K. Han and J. Jung, J. Chem. Phys. **125**, 084101 (2006).
[21] M. Akutsu, K. Koyasu, J. Atobe, N. Hosoya, K. Miyajima, M. Mitsui, and A. Nakajima, J. Phys. Chem. A **110**, 12073 (2006); K. Koyasu, M. Akutsu, J. Atobe, M. Mitsui, and A. Nakajima, Chem. Phys. Lett. **421**, 534 (2006).
[22] S. F. Li and X. G. Gong, Phys. Rev. B **74**, 045432 (2006).
[23] A. I. Boldyrev, J. Simons, X. Li, W. W. Chen, and L. S. Wang, J. Chem. Phys. **110**, 8980 (1999).
[24] A. I. Boldyrev, J. Simons, X. Li, and L. S. Wang, J. Chem. Phys. **111**, 4993 (1999).
[25] X. Li, L. S. Wang, A. I. Boldyrev, and J. Simons, J. Am. Chem. Soc. **121**, 6033 (1999).
[26] N. A. Cannon, A. I. Boldyrev, X. Li, and L. S. Wang, J. Chem. Phys. **113**, 2671 (2000).
[27] X. Li, H. F. Zhang, L. S. Wang, G. D. Geske, and A. I. Boldyrev, Angew. Chem., Int. Ed. **39**, 3630 (2000).
[28] X. Li, H. F. Zhang, L. S. Wang, A. E. Kuznetsov, N. A. Cannon, and A. I. Boldyrev, Angew. Chem., Int. Ed. **40**, 1867 (2001).
[29] A. E. Kuznetsov, A. I. Boldyrev, H. J. Zhai, X. Li, and L. S. Wang, J. Am. Chem. Soc. **124**, 11791 (2002).
[30] X. Li and L. S. Wang, Phys. Rev. B **65**, 153404 (2002).
[31] X. Li and L. S. Wang, Eur. Phys. J. D **34**, 9 (2005).
[32] B. B. Averkiev, A. I. Boldyrev, X. Li, and L. S. Wang, J. Chem. Phys. **125**, 124305 (2006).
[33] L. F. Cui, X. Li, and L. S. Wang, J. Chem. Phys. **124**, 054308 (2006).
[34] B. B. Averkiev, A. I. Boldyrev, X. Li, and L. S. Wang, J. Phys. Chem. A **111**, 34 (2007).
[35] T. Andersen, H. K. Haugen, and H. Hotop, J. Phys. Chem. Ref. Data **28**, 1511 (1999).
[36] L. S. Wang, H. S. Cheng, and J. Fan, J. Chem. Phys. **102**, 9480 (1995); L. S. Wang and H. Wu, in *Advances in Metal and Semiconductor Clusters. IV. Cluster Materials*, edited by M. A. Duncan (JAI, Greenwich, CT, 1998), pp. 299–343.
[37] S. Yoo and X. C. Zeng, Angew. Chem., Int. Ed. **44**, 1491 (2005).
[38] D. J. Wales and H. A. Scheraga, Science **285**, 1368 (1999); J. P. K. Doye and D. J. Wales, New J. Chem. **22**, 773 (1998).
[39] J. P. Perdew, K. Burke, and M. Ernzerhof, Phys. Rev. Lett. **77**, 3865 (1996).
[40] DMOL^3 is a density-functional theory program distributed by Accelrys, Inc.; B. Delley, J. Chem. Phys. **92**, 508 (1990).
[41] P. J. Hay and W. R. Wadt, J. Chem. Phys. **82**, 299 (1985).
[42] M. J. Frisch, G. W. Trucks, H. B. Schlegel, G. E. Scuseria, M. A. Robb, J. R. Cheeseman, V. G. Zakrzewski, J. A. Montgomery, R. E. Stratmann, J. C. Burant, S. Dapprich, J. M. Millam, A. D. Daniels, K. N. Kudin, M. C. Strain, O. Farkas, J. Tomasi, V. Barone, M. Cossi, R. Cammi, B. Mennucci, C. Pomelli, S. Clifford, J. Ochterski, G. A. Petersson, P. Y. Ayala, Q. Cui, K. Morokuma, D. K. Malick, A. D. Rabuck, K. Raghavachari, J. B. Foresman, J. Cioslowski, J. V. Ortiz, B. B. Stefanov, G. Liu, A. Liashenko, P. Piskorz, I. Komaromi, R. Gomperts, R. L. Martin, D. J. Fox, T. Keith, M. A. Al-Laham, C. Y. Peng, A. Nanayakkara, C. Gonzalez, M. Challacombe, P. M. W. Gill, B. G. Johnson, W. Chen, M. W. Wong, J. L. Andres, M. Head-Gordon, E. S. Replogle, and J. A. Pople, GAUSSIAN 03, revision C.02 Gaussian, Inc., Wallingford, CT, 2004.
[43] W. D. Knight, K. Clemenger, W. A. de Heer, W. A. Saunders, M. Y. Chou, and M. L. Cohen, Phys. Rev. Lett. **52**, 2141 (1984).
[44] C. Møller and M. S. Plesset, Phys. Rev. **46**, 618 (1934).